

Reactivity of Organolanthanide and Organolithium Complexes Containing the Guanidinate Ligands toward Isocyanate or Carbodiimide: Synthesis and Crystal Structures

Jie Zhang,* Xigeng Zhou, Ruifang Cai, and Linhong Weng

Department of Chemistry, Fudan University, Shanghai 200433, People's Republic of China

Received September 20, 2004

The direct reactions of $(C_5H_5)_2LnCl$ with $LiN=C(NMe_2)_2$ proceeded at room temperature in THF under pure nitrogen to yield the lanthanocene guanidinate complexes $[(C_5H_5)_2Ln(\mu-\eta^1:\eta^2-N=C(NMe_2)_2)]_2$ ($Ln = Gd$ (**1**), Er (**2**)). Treatment of phenyl isocyanate with complexes **1** and **2** results in monoinsertion of phenyl isocyanate into the $Ln-N(\mu-Gua)$ bond to yield the corresponding insertion products $[(C_5H_5)_2Ln(\mu-\eta^1:\eta^2-OC(N=C(NMe_2)_2)NPh)]_2$ ($Ln = Gd$ (**3**), Er (**4**)), presenting the first example of unsaturated organic small molecule insertion into the metal–guanidinate ligand bond. Further investigations indicate that *N,N*-diisopropylcarbodiimide does not react with complexes **1** and **2** under the same conditions; however, it readily inserts into the lithium–guanidinate ligand bond of $LiN=C(NMe_2)_2$. As a synthon of the insertion product $Li[(PrN)_2C(N=C(NMe_2)_2)]$, its reaction with $(C_5H_5)_2LnCl$ gives the novel organolanthanide complexes containing the guanidinoacetamidinate ligand, $(C_5H_5)_2Ln[(PrN)_2C(N=C(NMe_2)_2)]$ ($Ln = Yb$ (**5**), Er (**6**), Dy (**7**)). All complexes were characterized by elemental analysis and spectroscopic properties. The structures of complexes **1**, **3**, **5** and **7** were determined through X-ray single-crystal diffraction analysis.

Introduction

The search for new ligands to support metal complexes receives continual interest in inorganic chemistry and organometallic chemistry.^{1–3} Some efforts focus on the amidinate and guanidinate ligand systems, of which the steric bulk and electronic properties can be modified via variation of the organic substituents on the nitrogen atoms.^{2,3} More bonding modes of the guanidinate ligands than the amidinate ligands can be expected due to the third nitrogen chelating ability in the guanidinate system.³ Many organometallic guanidinate complexes were synthesized from across the periodic table in decades, where the guanidinate ligands do not participate in organometallic reactions, only as the typically supporting ligands to stabilize and construct these complexes.^{3–7} Recently, some investigations on the reactivities of the organometallic guanidinate complexes or the transformation of guanidinate ligands have been reported.^{8,9} However, to the best of our knowledge, no example of the insertion of

unsaturated organic small molecules into the metal–guanidinate ligand bonds was reported.

We have recently been interested in the reactivities of organolanthanide complexes toward unsaturated organic small molecules, providing many new methods for the $Ln-C$

* To whom correspondence should be addressed. E-mail: zhangjie@fudan.edu.cn.

- (1) (a) Britovsek, G. J. P.; Gibson, V. C.; Wass, D. F. *Angew. Chem., Int. Ed.* **1999**, *38*, 429. (b) Marques, N.; Sella, A.; Takats, J. *Chem. Rev.* **2002**, *102*, 2137.
- (2) Barker, J.; Kilner, M. *Coord. Chem. Rev.* **1994**, *133*, 219.
- (3) Bailey, P. J.; Pace, S. *Coord. Chem. Rev.* **2001**, *214*, 91.

- (4) (a) Ong, T. G.; Yap, G. P. A.; Richeson, D. S. *Organometallics* **2003**, *22*, 387. (b) Ong, T. G.; Yap, G. P. A.; Richeson, D. S. *Organometallics* **2002**, *21*, 2839. (c) Ong, T. G.; Wood, D.; Yap, G. P. A.; Richeson, D. S. *Organometallics* **2002**, *21*, 1. (d) Cotton, F. A.; Daniels, L. M.; Huang, P. L.; Murillo, C. *Inorg. Chem.* **2002**, *41*, 317. (e) Bazinet, P.; Wood, D.; Yap, G. P. A.; Richeson, D. S. *Inorg. Chem.* **2003**, *42*, 6225.
- (5) (a) Duncan, A. P.; Mullins, S. M.; Arnold, J.; Bergman, R. G. *Organometallics* **2001**, *20*, 1808. (b) Giesbrecht, G. R.; Whitener, G. D.; Arnold, J. *Organometallics* **2000**, *19*, 2809. (c) Okamoto, S.; Livinghouse, T. *Organometallics* **2000**, *19*, 1449. (d) Thiruphthi, N.; Yap, G. P. A.; Richeson, D. S. *J. Chem. Soc., Dalton Trans.* **1999**, 2947. (f) Bailey, P. J.; Grant, K. J.; Mitchell, L. A.; Pace, S.; Parkin, A.; Parsons, S. *J. Chem. Soc., Dalton Trans.* **1999**, 1887.
- (6) (a) Aelits, S. L.; Coles, M. P.; Swenson, D. G.; Jordan, R. F. *Organometallics* **1998**, *17*, 3265. (b) Chivers, T.; Parvez, M.; Schatte, G. *J. Organomet. Chem.* **1998**, *550*, 213. (c) Maia, J. R. da S.; Gazard, P. A.; Kilner, M.; Batsanova, A. S. *J. Chem. Soc., Dalton Trans.* **1997**, 4625. (d) Robinson, S. D.; Sahajpal, A. *J. Chem. Soc., Dalton Trans.* **1997**, 3349. (e) Bailey, P. J.; Bone, S. F.; Mitchell, L. A.; Parsons, S.; Taylor, K. J.; Yellowlees, L. J. *Inorg. Chem.* **1997**, *36*, 867. (f) Bailey, P. J.; Mitchell, L. A.; Parsons, S. *J. Chem. Soc., Dalton Trans.* **1996**, 2389. (g) Dinger, M. B.; Henderson, W. *Chem. Commun.* **1996**, 211. (h) Bailey, P. J.; Blake, A. L.; Kryszczuk, M.; Parsons, S.; Reed, D. *Chem. Commun.* **1995**, 1647.

or N bond transformation into Ln–N, Ln–O, and Ln–S bonds.¹⁰ Continuing our recent investigation of the lanthanide–ligand insertion and to learn more about the guanidinate anion as a ligand, we herein report the synthesis of two novel organolanthanide guanidinate complexes as well as their reactivities toward isocyanate, presenting the first example of 1,3-heteroculmene insertion into the metal–guanidinate ligand bonds. Furthermore, we also studied the reaction of $\text{LiN}=\text{C}(\text{NMe}_2)_2$ with carbodiimide. The insertion product can serve as a synthon to synthesize a series of novel organolanthanide complexes containing the guanidinoacetamidinate ligand.

Experimental Section

General Procedure. All operations involving air- and moisture-sensitive compounds were carried out under an inert atmosphere of purified argon or nitrogen using standard Schlenk techniques. The solvents THF, toluene, and *n*-hexane were refluxed and distilled over sodium benzophenone ketyl under nitrogen immediately prior to use. $(\text{C}_5\text{H}_5)_2\text{LnCl}^{1\text{a}}$ and $\text{LiN}=\text{C}(\text{NMe}_2)_2^{1\text{b}}$ were prepared by slightly modified literature methods, respectively. *N,N'*-Diisopropylcarbodiimide, phenyl isocyanate, and 1,1,3,3-tetramethylguanidine were purchased from Aldrich and were used without purification. Elemental analyses for C, H, and N were carried out on a Rapid CHN-O analyzer. Infrared spectra were obtained on a Nicolet FT-IR 360 spectrometer with samples prepared as Nujol mulls. Mass spectra were recorded on a Philips HP5989A instrument operating in EI mode. Crystalline samples of the respective complexes were rapidly introduced by the direct inlet techniques with a source temperature of 200 °C. The values of *m/z* refer to the isotopes ¹²C, ¹H, ¹⁴N, ¹⁶O, ¹⁵⁸Gd, ¹⁶⁴Dy, ¹⁶⁶Er, and ¹⁷⁴Yb.

Synthesis of $[(\text{C}_5\text{H}_5)_2\text{Gd}(\mu\text{-}\eta^1\text{-}\eta^2\text{-N}=\text{C}(\text{NMe}_2)_2)]_2$ (1). A solution of $\text{Li}[\text{N}=\text{C}(\text{NMe}_2)_2]$ (0.151 g, 1.24 mmol) was added dropwise to a 30 mL THF solution of $(\text{C}_5\text{H}_5)_2\text{GdCl}$ (0.400 g, 1.24 mmol) at room temperature. After stirring for 24 h, the solvent was removed under vacuum, and the solid residue was extracted with 30 mL of toluene. The pale yellow extract solution was concentrated and cooled at –20 °C to give a colorless powder. Recrystallization of the powder from a mixture of THF and toluene gave **1** as colorless crystals. Yield: 0.385 g (71%). Anal. Calcd for $\text{C}_{34}\text{H}_{52}\text{N}_6\text{OGd}_2$: C, 46.66; H, 5.98; N, 9.60. Found: C, 46.59; H, 5.93; N, 9.67. IR (Nujol, cm^{-1}): 3175 w, 1606 s, 1581 m, 1550 w, 1306 m, 1258 s, 1155 s, 1082 s, 1009 s, 977 m, 890 s, 841 m, 759 m, 693 w, 664 m. EI-MS: *m/z* [fragment, relative intensity (%)] = 402 (^{1/2}M, 14),

387 (^{1/2}M – CH₃, 29), 288 (Cp₂Gd, 46), 115 (L + H, 23), 72 (THF, 17), 65 (Cp, 72) [L = NC(NMe₂)₂].

Synthesis of $[(\text{C}_5\text{H}_5)_2\text{Er}(\mu\text{-}\eta^1\text{-}\eta^2\text{-N}=\text{C}(\text{NMe}_2)_2)]_2$ (2). Following the procedure described for **1**, reaction of $(\text{C}_5\text{H}_5)_2\text{ErCl}$ (0.557 g, 1.68 mmol) with $\text{Li}[\text{N}=\text{C}(\text{NMe}_2)_2]$ (0.203 g, 1.68 mmol) gave **2** as pink crystals. Yield: 0.504 g (67%). Anal. Calcd for $\text{C}_{34}\text{H}_{52}\text{N}_6\text{OEr}_2$: C, 45.61; H, 5.85; N, 9.39. Found: C, 45.39; H, 5.71; N, 9.47. IR (Nujol, cm^{-1}): 3175 w, 1607 s, 1541 m, 1297 m, 1155 s, 1070 s, 1009 s, 890 s, 759 m, 662 m. EI-MS: *m/z* [fragment, relative intensity (%)] = 410 (^{1/2}M, 7), 395 (^{1/2}M – CH₃, 16), 296 (Cp₂Er, 54), 115 (L + H, 33), 72 (THF, 23), 65 (Cp, 69) [L = NC(NMe₂)₂].

Synthesis of $[(\text{C}_5\text{H}_5)_2\text{Gd}(\mu\text{-}\eta^1\text{-}\eta^2\text{-OC}(\text{N}=\text{C}(\text{NMe}_2)_2)\text{NPh})]_2$ (3). To a 20 mL THF solution of **1** (0.341 g, 0.39 mmol) was slowly added phenyl isocyanate (0.094 g, 0.79 mmol) dropwise at room temperature, and the mixture stirred for 12 h. The reaction solution was concentrated to ca. 3 mL by reduced pressure, and colorless crystals of **3** were obtained at –20 °C for several days. Yield: 0.203 g (44%). Anal. Calcd for $\text{C}_{52}\text{H}_{70}\text{N}_8\text{O}_4\text{Gd}_2$: C, 52.68; H, 5.95; N, 9.45. Found: C, 52.63; H, 5.98; N, 9.61. IR (Nujol, cm^{-1}): 3170 w, 1598 s, 1557 s, 1500 m, 1423 m, 1410 w, 1313 m, 1238 s, 1233 s, 1154 m, 1054 s, 1012 s, 985 s, 920 s, 866 s, 774 s, 694 s, 665 w. EI-MS: *m/z* [fragment, relative intensity (%)] = 977 (M – Cp, 3), 912 (M – 2Cp, 1), 521 (^{1/2}M, 29), 506 (^{1/2}M – CH₃, 23), 456 (^{1/2}M – Cp, 17), 288 (Cp₂Gd, 54), 233 (L, 43), 120 (L – NC(NMe₂)₂ + H, 37) [L = OC(NC(NMe₂)₂)NPh].

Synthesis of $[(\text{C}_5\text{H}_5)_2\text{Er}(\mu\text{-}\eta^1\text{-}\eta^2\text{-OC}(\text{N}=\text{C}(\text{NMe}_2)_2)\text{NPh})]_2$ (4). Following the procedure described for **3**, reaction of **2** (0.421 g, 0.47 mmol) with phenyl isocyanate (0.112 g, 0.94 mmol) gave **4** as pink crystals. Yield: 0.289 g (51%). Anal. Calcd for $\text{C}_{52}\text{H}_{70}\text{N}_8\text{O}_4\text{Er}_2$: C, 51.80; H, 5.85; N, 9.29. Found: C, 51.68; H, 5.91; N, 9.37. IR (Nujol, cm^{-1}): 3170 w, 1598 s, 1557 s, 1500 m, 1423 m, 1410 w, 1313 m, 1238 s, 1233 s, 1154 m, 1072 m, 1054 s, 1012 s, 985 s, 919 s, 866 s, 810 m, 774 s, 761 m, 694 s, 665 w. EI-MS: *m/z* [fragment, relative intensity (%)] = 529 (^{1/2}M, 16), 514 (^{1/2}M – CH₃, 42), 464 (^{1/2}M – Cp, 21), 296 (Cp₂Er, 38), 233 (L, 44), 120 (L – NC(NMe₂)₂ + H, 29) [L = OC(NC(NMe₂)₂)NPh].

Synthesis of $(\text{C}_5\text{H}_5)_2\text{Yb}[(\text{PrN})_2\text{C}(\text{N}=\text{C}(\text{NMe}_2)_2)]$ (5). To a 15 mL THF solution of $\text{Li}[\text{N}=\text{C}(\text{NMe}_2)_2]$ (0.108 g, 0.89 mmol) was slowly added *N,N'*-diisopropylcarbodiimide (0.112 g, 0.89 mmol) dropwise at room temperature. After stirring for 12 h, the mixture was added into the 20 mL THF solution of $(\text{C}_5\text{H}_5)_2\text{YbCl}$ (0.301 g, 0.89 mmol) at room temperature, and the solution stirred for 12 h. Then, the solvent was removed under vacuum, and the solid residue was extracted with 30 mL of toluene. Recrystallization from a mixture of THF and toluene gave **5** as red crystals. Yield: 0.295 g (61%). Anal. Calcd for $\text{C}_{22}\text{H}_{36}\text{N}_5\text{Yb}$: C, 48.61; H, 6.67; N, 12.88. Found: C, 48.54; H, 6.63; N, 12.97. IR (Nujol, cm^{-1}): 3175 w, 1605 s, 1558 w, 1301 m, 1227 m, 1142 s, 1064 m, 1014 s, 963 m, 923 s, 892 s, 768 s, 663 m. EI-MS: *m/z* [fragment, relative intensity (%)] = 544 (M, 9), 529 (M – CH₃, 35), 304 (Cp₂Yb, 10), 241 (L + H, 29), 196 (L – NMe₂, 13), 183 (L – NⁱPr, 67), 141 (L – C(NMe₂)₂ + H, 100) [L = (ⁱPrN)₂C(N=C(NMe₂)₂)].

Synthesis of $(\text{C}_5\text{H}_5)_2\text{Er}[(\text{PrN})_2\text{C}(\text{N}=\text{C}(\text{NMe}_2)_2)]$ (6). Following the procedure described for **5**, reaction of *N,N'*-diisopropylcarbodiimide (0.158 g, 1.25 mmol) with $\text{Li}[\text{N}=\text{C}(\text{NMe}_2)_2]$ (0.151 g, 0.78 mmol) and subsequently with $(\text{C}_5\text{H}_5)_2\text{ErCl}$ (0.416 g, 1.25 mmol) gave **6** as pink crystals. Yield: 0.430 g (64%). Anal. Calcd for $\text{C}_{22}\text{H}_{36}\text{N}_5\text{Er}$: C, 49.41; H, 6.78; N, 13.10. Found: C, 49.31; H, 6.75; N, 13.14. IR (Nujol, cm^{-1}): 3175 w, 1604 s, 1559 w, 1300 m, 1222 m, 1140 s, 1058 m, 1012 s, 956 m, 923 s, 893 s, 763 s, 663 m. EI-MS: *m/z* [fragment, relative intensity (%)] = 536 (M, 17), 521 (M – CH₃, 54), 296 (Cp₂Er, 43), 241 (L + H, 26), 196

- (7) (a) Lu, Z.; Yap, G. P. A.; Richeson, D. S. *Organometallics* **2001**, *20*, 706. (b) Zhou, Y.; Yap, G. P. A.; Richeson, D. S. *Organometallics* **1998**, *17*, 4387.
 (8) (a) Luo, Y. J.; Yao, Y. M.; Shen, Q. *Macromolecules* **2002**, *35*, 8670. (b) Kretschmer, W. P.; Dijkhuis, C.; Meetsma, A.; Hessen, B.; Teuben, J. H. *Chem. Commun.* **2002**, 608. (c) Ong, T. G.; Yap, G. P. A.; Richeson, D. S. *J. Am. Chem. Soc.* **2003**, *125*, 8100.
 (9) (a) Ong, T. G.; Yap, G. P. A.; Richeson, D. S. *Chem. Commun.* **2003**, 2612. (b) Foley, S. R.; Yap, G. P. A.; Richeson, D. S. *Chem. Commun.* **2000**, 1515. (c) Foley, S. R.; Yap, G. P. A.; Richeson, D. S. *Inorg. Chem.* **2002**, *41*, 4149. (d) Thirupathi, N.; Yap, G. P. A.; Richeson, D. S. *Organometallics* **2000**, *19*, 2573.
 (10) (a) Zhang, J.; Cai, R. F.; Weng, L. H.; Zhou, X. G. *Organometallics* **2004**, *23*, 3303. (b) Zhang, J.; Cai, R. F.; Weng, L. H.; Zhou, X. G. *Organometallics* **2003**, *22*, 5385. (c) Zhang, J.; Cai, R. F.; Weng, L. H.; Zhou, X. G. *J. Organomet. Chem.* **2003**, *672*, 94. (d) Zhang, J.; Ruan, R. Y.; Shao, Z. H.; Cai, R. F.; Weng, L. H.; Zhou, X. G. *Organometallics* **2002**, *21*, 1420.
 (11) (a) Magin, R. E.; Manastyrskij, S.; Dubeck, M. *J. Am. Chem. Soc.* **1963**, *85*, 672. (b) Pattison, I.; Wade, K.; Wyatt, B. K. *J. Chem. Soc. A* **1968**, 837.

Table 1. Crystal and Data Collection Parameters of Complexes **1**, **3**, **5**, and **7**

	1	3	5	7
formula	C ₃₄ H ₅₂ N ₆ O ₄ Gd ₂	C ₅₂ H ₇₀ N ₈ O ₄ Gd ₂	C ₂₂ H ₃₆ N ₅ Yb	C ₂₂ H ₃₆ N ₅ Dy
mol wt	875.32	1185.66	543.60	533.06
cryst color	colorless	colorless	orange	pale yellow
crystal dimens (mm ³)	0.45 × 0.20 × 0.15	0.30 × 0.20 × 0.15	0.20 × 0.10 × 0.05	0.25 × 0.20 × 0.08
cryst syst	orthorhombic	triclinic	triclinic	triclinic
space group	<i>Pccn</i>	<i>P</i> $\bar{1}$	<i>P</i> $\bar{1}$	<i>P</i> $\bar{1}$
unit cell dimensions				
<i>a</i> (Å)	14.626(5)	8.865(3)	9.686(4)	9.749(3)
<i>b</i> (Å)	15.245(5)	10.953(3)	10.351(4)	10.425(3)
<i>c</i> (Å)	16.531(5)	13.984(4)	13.230(5)	13.309(4)
α (deg)		97.327(4)	72.912(5)	73.275(4)
β (deg)	3686(2)	92.531(4)	70.051(4)	70.142(4)
γ (deg)		100.162(4)	83.910(5)	84.204(4)
<i>V</i> (Å ³)		1322.5(6)	1191.8(8)	1218.4(6)
<i>Z</i>	4	1	2	2
<i>D_c</i> (g·cm ⁻³)	1.577	1.489	1.515	1.453
μ (mm ⁻¹)	3.600	2.535	3.939	3.082
<i>F</i> (000)	1736	598	546	538
radiation	Mo K α	Mo K α	Mo K α	Mo K α
($\lambda = 0.710730$ Å)				
<i>T</i> (K)	298.2	293.2	293.2	298.2
scan type	$\omega-2\theta$	$\omega-2\theta$	$\omega-2\theta$	$\omega-2\theta$
θ range (deg)	1.93–26.01	1.47–25.01	1.70–25.01	1.69–26.01
<i>h, k, l</i> range	–18 ≤ <i>h</i> ≤ 18, –18 ≤ <i>k</i> ≤ 7 –19 ≤ <i>l</i> ≤ 20	–10 ≤ <i>h</i> ≤ 10 –11 ≤ <i>k</i> ≤ 13 –16 ≤ <i>l</i> ≤ 14	–10 ≤ <i>h</i> ≤ 11 –6 ≤ <i>k</i> ≤ 12 –14 ≤ <i>l</i> ≤ 15	–8 ≤ <i>h</i> ≤ 12 –10 ≤ <i>k</i> ≤ 12 –15 ≤ <i>l</i> ≤ 16
no. reflns measured	15906	5541	4967	5600
no. unique reflns	3623 (<i>R</i> _{int} = 0.0361)	4580 (<i>R</i> _{int} = 0.0163)	4106 (<i>R</i> _{int} = 0.0181)	4683 (<i>R</i> _{int} = 0.0141)
completeness to θ	99.9% ($\theta = 26.01$)	98.3% ($\theta = 25.01$)	97.9% ($\theta = 25.01$)	97.5% ($\theta = 26.01$)
max and min transm	0.6142 and 0.3269	0.7023 and 0.5168	0.8274 and 0.5063	0.7906 and 0.5130
refinement method	<i>a</i>	<i>a</i>	<i>a</i>	<i>a</i>
data/restraints/params	3623/2/199	4580/7/273	4106/0/261	4683/0/261
GOF on <i>F</i> ²	1.036	1.025	1.143	1.037
final <i>R</i> indices [<i>I</i> > 2 σ (<i>I</i>)]	<i>R</i> ₁ = 0.0494, <i>wR</i> ₂ = 0.0990	<i>R</i> ₁ = 0.0325, <i>wR</i> ₂ = 0.0843	<i>R</i> ₁ = 0.0340, <i>wR</i> ₂ = 0.0894	<i>R</i> ₁ = 0.0266, <i>wR</i> ₂ = 0.0578
<i>R</i> indices (all data)	<i>R</i> ₁ = 0.0610, <i>wR</i> ₂ = 0.1051	<i>R</i> ₁ = 0.0361, <i>wR</i> ₂ = 0.0875	<i>R</i> ₁ = 0.0388, <i>wR</i> ₂ = 0.0911	<i>R</i> ₁ = 0.0307, <i>wR</i> ₂ = 0.0595
largest diff peak and hole (e ⁻ ·Å ⁻³)	1.039 and –0.843	1.085 and –0.544	1.473 and –1.011	0.738 and –0.517

^a Full-matrix least-squares on *F*².

(L – NMe₂, 18), 183 (L – NⁱPr, 64), 141 (L – C(NMe₂)₂ + H, 95) [L = (i-PrN)₂C(N=C(NMe₂)₂)].

Synthesis of (C₅H₅)₂Dy[(i-PrN)₂C(N=C(NMe₂)₂)] (7**).** Following the procedure described for **5**, reaction of *N,N'*-diisopropylcarbo-diimide (0.143 g, 1.13 mmol) with Li[N=C(NMe₂)₂] (0.137 g, 1.13 mmol) and subsequently with (C₅H₅)₂DyCl (0.371 g, 1.13 mmol) gave **7** as pink crystals. Yield: 0.476 g (79%). Anal. Calcd for C₂₂H₃₆N₅Dy: C, 49.57; H, 6.80; N, 13.14. Found: C, 49.53; H, 6.69; N, 13.09. IR (Nujol, cm⁻¹): 3170 w, 1606 s, 1301 m, 1225 m, 1143 s, 1064 m, 1010 s, 963 m, 926 s, 890 s, 764 s, 664 m. EI-MS: *m/z* [fragment, relative intensity (%)] = 534 (M, 8), 519 (M – CH₃, 30), 304 (Cp₂Dy, 22), 241 (L + H, 9), 196 (L – NMe₂, 8), 183 (L – NⁱPr, 43), 141 (L – C(NMe₂)₂ + H, 69) [L = (i-PrN)₂C(N=C(NMe₂)₂)].

X-ray Data Collection, Structure Determination, and Refinement. Suitable single crystals of complexes **1**, **3**, **5**, and **7** were sealed under argon in Lindemann glass capillaries for X-ray structural analysis. Diffraction data were collected on a Bruker SMART Apex CCD diffractometer using graphite-monochromated Mo K α ($\lambda = 0.71073$ Å) radiation. During the intensity data collection, no significant decay was observed. The intensities were corrected for Lorentz-polarization effects and empirical absorption with the SADABS program.¹² The structures were solved by the direct method using the SHELXL-97 program.¹³ All non-hydrogen

atoms were found from the difference Fourier syntheses. The H atoms were included in calculated positions with isotropic thermal parameters related to those of the supporting carbon atoms, but were not included in the refinement. All calculations were performed using the Bruker Smart program. A summary of the crystallographic data and selected experimental information are given in Table 1.

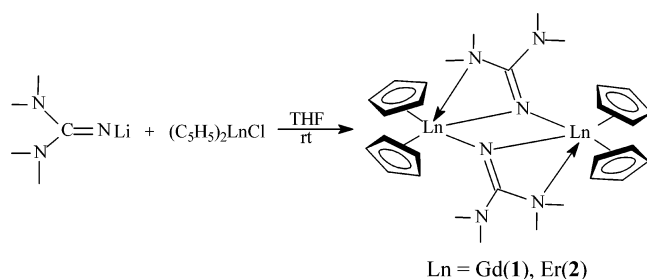
Results and Discussion

Synthesis and Characterizations of the Lanthanocene Guanidinate Complexes [(C₅H₅)₂Ln(μ - η^1 : η^2 -N=C(NMe₂)₂)₂] (Ln = Gd(1**), Er(**2**)).** Although the synthesis of the guanidinate complex LiN=C(NMe₂)₂ was reported early on as the first monoanionic guanidinate complex in 1968,^{11b} the effort on the reactivity of the complex is very limited.¹⁴ In order to investigate the bonding mode of the guanidinate ligand to rare earth metal ion, we synthesized two organo-lanthanide guanidinate complexes [(C₅H₅)₂Ln(μ - η^1 : η^2 -N=C(NMe₂)₂)₂] (Ln = Gd(**1**), Er(**2**)) by the reactions of (C₅H₅)₂LnCl with LiN=C(NMe₂)₂ in THF at room temperature (Scheme 1).

(13) Sheldrick, G. M. *SHELXL-97, Program for the refinement of the crystal structure*; University of Göttingen: Göttingen, Germany, 1997.

(14) (a) Clegg, W.; Snaith, R.; Shearer, H. M. M.; Wade, K.; Whitehead, G. *J. Chem. Soc., Dalton Trans.* **1983**, 1309. (b) Stalke, D.; Paver, M. A.; Wright, D. S. *Angew. Chem., Int. Ed. Engl.* **1993**, 32, 428.

Scheme 1



Both of the complexes are air- and moisture-sensitive. They are soluble in THF and toluene and slightly soluble in *n*-hexane. Complexes **1** and **2** have been characterized by elemental analysis and infrared and mass spectroscopies, which were in good agreement with the proposed structures. The mass spectra show that both of them are characterized by the molecule ion peaks and a series of peaks clearly representing fragments derived from the parent molecules. In the IR spectra, complexes **1** and **2** exhibit the characterized absorptions at 1610 cm^{-1} , which can be attributed to the bridged-chelating guanidinate ligand.¹⁴ The structure of **1** was also identified by X-ray single-crystal diffraction analysis, which reveals an unusual bonding mode of the guanidinate ligand with the central metal ion (Figure 1).

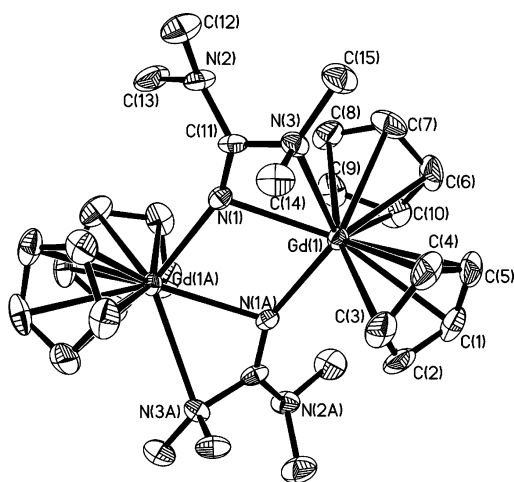


Figure 1. ORTEP diagram of **1** with the probability ellipsoids drawn at the 30% level. Hydrogen atoms omitted for clarity.

The crystal structure of complex **1** reveals a solvent-free centrosymmetric dimer. Selected bond distances and angles are compiled in Table 2. The X-ray analysis shows an unusual bonding mode of the guanidinate ligand $\text{N}=\text{C}(\text{NMe}_2)_2$, which acts both as a bridging and a chelating group. Each gadolinium atom is coordinated by two η^5 -cyclopentadienyl groups, one chelating η^2 -guanidinate ligand, and one bridging nitrogen atom from another guanidinate ligand, to form a distorted octahedral geometry. The unique character of complex **1** is that the coplanarity of the four-membered set $\text{Gd}-\text{N}-\text{C}-\text{N}$ is destroyed. The dihedral angle between the planes of $\text{N}(1)-\text{Gd}(1)-\text{C}(11)$ and $\text{N}(3)-\text{Gd}(1)-\text{C}(11)$ is 148.16° . This is very different from the organolanthanide guanidinate complexes $(\text{C}_5\text{H}_5)_2\text{Ln}[\text{N}(\text{C}(\text{NMe}_2)_2)\text{N}(\text{Pr})]$ ($\text{Ln} = \text{Yb}, \text{Y}, \text{Dy}$),^{10a,c} of which the corresponding moiety

Table 2. Bond Lengths (Å) and Angles (deg) for **1**

Gd(1)–N(1A)	2.308(6)	Gd(1)–C(7)	2.744(9)
Gd(1)–N(1)	2.420(5)	Gd(1)–C(2)	2.751(7)
Gd(1)–C(9)	2.695(8)	Gd(1)–C(6)	2.754(8)
Gd(1)–C(10)	2.702(8)	Gd(1)–C(11)	2.880(8)
Gd(1)–C(4)	2.717(8)	N(1)–C(11)	1.247(8)
Gd(1)–N(3)	2.721(6)	N(1)–Gd(1A)	2.308(6)
Gd(1)–C(3)	2.728(8)	N(2)–C(11)	1.381(9)
Gd(1)–C(8)	2.735(8)	N(2)–C(13)	1.446(11)
Gd(1)–C(5)	2.740(8)	N(3)–C(11)	1.452(9)
N(1A)–Gd(1)–N(1)	74.6(2)	N(1)–C(11)–N(3)	117.4(6)
C(11)–N(1)–Gd(1A)	154.5(5)	N(2)–C(11)–N(3)	116.3(6)
C(11)–N(1)–Gd(1)	98.4(5)	N(1)–C(11)–Gd(1)	56.2(4)
Gd(1A)–N(1)–Gd(1)	105.3(2)	N(2)–C(11)–Gd(1)	148.2(5)
C(11)–N(3)–Gd(1)	81.1(4)	N(3)–C(11)–Gd(1)	69.0(4)
N(1)–C(11)–N(2)	126.1(7)		

is coplanar. Consistent with this, the distance of $\text{N}(3)-\text{C}(11)$ ($1.452(9)\text{ Å}$) is significantly elongated, longer than the distance of $\text{N}(2)-\text{C}(11)$ ($1.381(9)\text{ Å}$). It may be attributed to the interactions of the rare earth metal ions with the chelating nitrogen atoms. The bond length of $\text{N}(1)-\text{C}(11)$ ($1.247(8)\text{ Å}$) is comparable to the value accepted for the $\text{N}(\text{sp}^2)=\text{C}(\text{sp}^2)$ double bond (1.26 Å).¹⁵

Significantly, it is different from the results observed in the bridging-coordination metal guanidates, where two bridging $\text{M}-\text{N}$ distances are usually similar,¹⁴ in that the $\text{Gd}(1)-\text{N}(1\text{A})$ distance of $2.308(6)\text{ Å}$ in **1** is significantly longer than the $\text{Gd}(1)-\text{N}(1)$ distance of $2.420(5)\text{ Å}$. The latter is within the range of the $\text{Ln}-\text{N}$ donor bonds. It may be attributed to the steric effects caused by the chelating coordination of Gd^{3+} to the guanidinate ligand. There is a weak interaction between $\text{Gd}(1)$ with $\text{C}(11)$.¹⁶ The $\text{Gd}-\text{C}(\text{Cp})$ distances range from $2.695(8)$ to $2.754(8)\text{ Å}$ and are in the normal ranges observed for lanthanocene complexes. The average $\text{Gd}-\text{C}(\text{Cp})$ distance of $2.729(8)\text{ Å}$ is similar to those found in other Cp_2Gd -containing compounds, such as $[(\text{C}_5\text{H}_5)_2\text{Gd}(\mu-\eta^2\text{-ONCMe}_2)]_2$, $2.68(2)\text{ Å}$;^{17a} $[(\text{C}_5\text{H}_5)_2\text{GdCl}]_4$, $2.67(4)\text{ Å}$.^{17b}

Reaction of Complexes **1** and **2** with Phenyl Isocyanate.

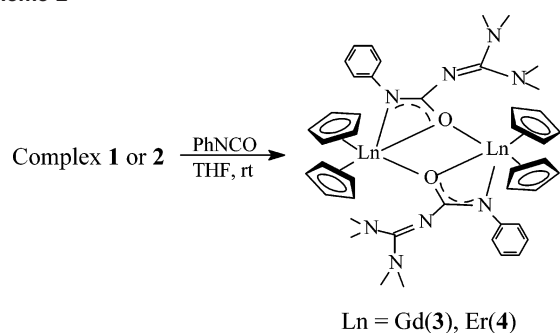
Although organometallic guanidates have been extensively investigated,^{8,9} no example of the $\text{M}-\text{N}$ insertion based on the guanidinate ligand was reported. To further investigate the effects of the steric factors and bonding mode of the nitrogen ligand on the insertion, reactions of the organolanthanide guanidates **1** and **2** with phenyl isocyanate (PhNCO) or N,N' -diisopropylcarbodiimide ($\text{PrN}=\text{C}=\text{N}(\text{Pr})$) have been studied. The results indicate that PhNCO can monoinsert into the $\text{Ln}-\text{N}$ ($\mu-\eta^1:\eta^2$ -guanidinate) bond of **1** and **2** to yield $[(\text{C}_5\text{H}_5)_2\text{Ln}(\mu-\eta^1:\eta^2\text{-OC}(\text{N}=\text{C}(\text{NMe}_2)_2)\text{NPh})]_2$ ($\text{Ln} = \text{Gd}$ (**3**), Er (**4**)) (Scheme 2), but no further reaction involving phenyl isocyanate was observed in the presence of excess PhNCO even with a higher reaction temperature and a longer reaction time. This is different from the observation in the reaction of PhNCO with the organolanthanide amidinate complex

(15) Mullins, S. M.; Duncan, A. P.; Bergman, R. G.; Arnold, J. *Inorg. Chem.* **2001**, *40*, 6952 and references therein.

(16) Zhou, X. G.; Zhang, L. B.; Zhu, M.; Cai, R. F.; Weng, L. H. *Organometallics* **2001**, *20*, 5700.

(17) (a) Wu, Z. Z.; Zhou, X. G.; Zhang, W.; Xu, Z.; You, X. Z.; Huang, X. Y. *J. Chem. Soc., Chem. Commun.* **1994**, 813. (b) Lamberts, W.; Hessner, B.; Lueken, H. *Inorg. Chim. Acta* **1987**, *139*, 215.

Scheme 2



$(C_5H_5)_2Y[{}^iBuNC({}^tBu)N{}^iBu]$, where PhNCO can be catalyzed to cyclotrimerization.^{10d} It may be attributed to the differences of the steric hindrance and the bonding mode between **3** and $(C_5H_5)_2Y[{}^iBuNC({}^tBu)N{}^iBu]$; where complex **3** acts in both bridging and chelating modes, the latter acts as only a chelating mode, as shown in Figure 2 (vide infra).

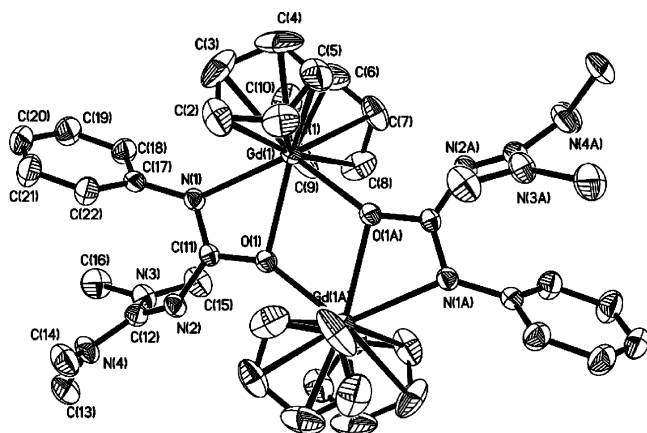


Figure 2. ORTEP diagram of **3** with the probability ellipsoids drawn at the 30% level. Hydrogen atoms omitted for clarity.

In contrast to organolanthanide amido complexes,^{10a–c} complexes **1** and **2** do not react with *N,N'*-diisopropylcarbodiimide under the same conditions. This may be attributed to the $\mu\text{-}\eta^1\text{:}\eta^2$ -bonding mode of the guanidinate ligand. Such a bonding structure results in a decrease in the Ln–N bond reactivity and is disfavored for the interaction of the carbodiimide molecule with the central metal.^{10b}

The mass spectra of complexes **3** and **4** display the molecular ion peaks and the insertion fragments of $[OC(N=C(NMe_2)_2)NPh]$. These complexes show an additional band in the IR spectra at 1598 cm^{-1} , corresponding to the characterized delocalized $-\text{O}\cdot\text{C}\cdot\text{N}-$ stretching mode.¹⁶

X-ray determination indicates that complex **3** has a dimeric structure, as shown in Figure 2, in which $(C_5H_5)_2Gd$ fragments connect with two $[OC(N=C(NMe_2)_2)NPh]^-$ units. The eight atoms Gd(1), N(1), C(11), O(1), Gd(1A), N(1A), C(11A), and O(1A) form an interlinked tricyclic structure via two bridged O atoms. Its coordination geometry is similar to that in complex $[(CH_3C_5H_4)_2Ln(OC(R)NPh)]_2$ ($R = {}^iBu$, $Ln = Sm, Ho$; $R = Np, Ln = Dy$).¹⁶ Selected bond distances and angles are given in Table 3. The N(1)–C(11) and O(1)–C(11) bond lengths, 1.306(6) and 1.318(5) Å, are in intermediate values between with the corresponding C–N

Table 3. Bond Lengths (Å) and Angles (deg) for **3**

Gd(1)–O(1A)	2.315(3)	Gd(1)–C(11)	2.906(6)
Gd(1)–O(1)	2.427(3)	N(1)–C(11)	1.306(6)
Gd(1)–N(1)	2.459(4)	N(1)–C(17)	1.420(6)
Gd(1)–C(10)	2.670(7)	N(2)–C(12)	1.305(6)
Gd(1)–C(9)	2.681(6)	N(2)–C(11)	1.359(6)
Gd(1)–C(5)	2.682(6)	N(3)–C(12)	1.359(7)
Gd(1)–C(3)	2.683(7)	N(4)–C(12)	1.371(7)
Gd(1)–C(6)	2.692(7)	N(4)–C(13)	1.446(7)
Gd(1)–C(8)	2.697(6)	N(4)–C(14)	1.461(8)
Gd(1)–C(4)	2.695(7)	O(1)–C(11)	1.318(5)
Gd(1)–C(7)	2.714(6)	O(1)–Gd(1A)	2.315(3)
Gd(1)–C(1)	2.725(6)		
C(11)–N(1)–Gd(1)	96.2(3)	O(1)–C(11)–N(2)	116.9(4)
C(17)–N(1)–Gd(1)	138.9(3)	N(1)–C(11)–Gd(1)	57.3(2)
C(12)–N(2)–C(11)	124.0(4)	O(1)–C(11)–Gd(1)	55.9(2)
C(11)–O(1)–Gd(1A)	148.7(3)	N(2)–C(11)–Gd(1)	170.5(3)
C(11)–O(1)–Gd(1)	97.3(3)	N(2)–C(12)–N(3)	124.6(5)
Gd(1A)–O(1)–Gd(1)	112.6(1)	N(2)–C(12)–N(4)	118.9(5)
N(1)–C(11)–O(1)	113.1(4)	N(3)–C(12)–N(4)	116.3(5)
N(1)–C(11)–N(2)	129.8(4)		

and C–O single- and double-bond distances. These bond parameters indicate substantial electronic delocalization over the O–C–N unit.^{16,18} Consistent with this, the observed Gd–N(1) (2.459(4) Å) bond distance is in agreement with that of the Sm–N(1A) (2.515(3) Å) in $[(CH_3C_5H_4)_2Sm(OC({}^iBu)NPh)]_2$,¹⁶ if the difference in ionic radii is considered. The Gd(1)–O(1) distance of 2.427(3) Å in **3** is significantly longer than the Gd(1)–O(1A) distance of 2.315(3) Å. The average Gd–O bond distance, 2.371(3) Å, is comparable to the corresponding values found in $[(CH_3C_5H_4)_2Sm(OC({}^iBu)NPh)]_2$ (Sm–O 2.452(3) Å),¹⁶ if the difference in ionic radii is considered.¹⁹

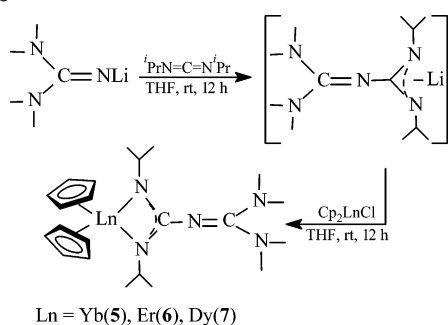
It should be noted that the C=N double-bond distance (N(2)–C(12) 1.305(6) Å) of the guanidine group $N=C(NMe_2)_2$ in **3**, which is comparable to the delocalized N(1)–C(11) bond distance (1.306(6) Å), is significantly longer than the corresponding value (N(1)–C(11) 1.247(8) Å) found in **1**. The latter is the typical value for $N(sp^2)=C(sp^2)$ double bond (1.26 Å).¹⁵ It may be attributed that the π electron part of the guanidine group takes part in conjugated interaction of the Gd–O–C–N unit. The Gd–C(Cp) distances in **3** are also in the normal ranges.¹⁷

Synthesis and Characterizations of the Organolanthanide Derivates Containing Guanidinoacetamidinate Ligand, $(C_5H_5)_2Ln[({}^iPrN)_2C(N=C(NMe_2)_2)]$ ($Ln = Yb$ (5**), Er (**6**), Dy (**7**)).** Although *N,N'*-diisopropylcarbodiimide cannot react with complexes **1** and **2** to give the corresponding insertion products, its reaction with $Li[N=C(NMe_2)_2]$ gives the insertion intermediate product, which can be used as a synthon to synthesize other organometallic complexes containing guanidinoacetamidinate ligand. Treatment of *N,N'*-diisopropylcarbodiimide with $Li[N=C(NMe_2)_2]$ and subsequently with $(C_5H_5)_2LnCl$ in THF at room temperature gave $(C_5H_5)_2Ln[({}^iPrN)_2C(N=C(NMe_2)_2)]$ ($Ln = Yb$ (**5**), Er (**6**), Dy (**7**)), as shown in Scheme 3. Insertions of carbodiimide into the alkali metal M–N bonds have been investigated,²⁰ providing an effective method of synthesis of metal guanidi-

(18) Allen, F. H.; Kennard, O.; Watson, D. G.; Brammer, L.; Orpen, A. G. *J. Chem. Soc., Perkin Trans.* **1987**, S1.

(19) Shannon, R. D. *Acta Crystallogr.* **1976**, A32, 751.

Scheme 3



nate complexes via the metathesis reaction of MCl_x with the guanidinate alkali metal salts. However, to the best of our knowledge, no example of the insertion of carbodiimide into the lithium–guanidinate ligand bond has been reported. Our results indicate that carbodiimide readily inserts into the lithium–guanidinate ligand bond.

These compounds have been characterized by standard spectroscopic and analytical techniques. Complexes **5** and **7** have also been structurally characterized by X-ray analysis.

The X-ray structural analysis results show that **5** (Figure 3, Table 4) is a solvent-free monomer with the ytterbium

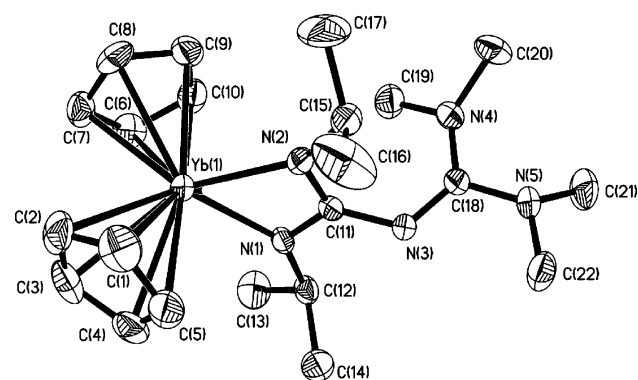


Figure 3. ORTEP diagram of **5** with the probability ellipsoids drawn at the 30% level. Hydrogen atoms omitted for clarity.

atom bonded to two η^5 -cyclopentadienyl rings and one chelating guanidinoacetamidinate ligand $[(^i\text{PrN})_2\text{C}(\text{N}=\text{C}(\text{NMe}_2)_2)]$ to form distorted tetrahedron geometry similar to the lanthanocene guanidinates $(\text{C}_5\text{H}_5)_2\text{Ln}[(^i\text{PrNC}(\text{N}^i\text{Pr}_2)\text{N}^i\text{Pr}]]$ (Ln = Yb, Dy).^{10c} The coordination number of the central Yb^{3+} is eight. As expected, the coordinated guanidinoacetamidinate group forms essentially a planar four-membered ring with the Yb atom within experimental errors. The bond angles around C(11) are consistent with sp^2 hybridization. The cent–Yb–cent (cent = the center of cyclopentadienyl ring) plane relative to the YbNCN plane is approximately perpendicular. This disposition may result from the steric interaction between two bulky isopropyl groups and two cyclopentadienyl ligands. The $\text{C}(11)\text{--N}(1)$ (1.343(8) Å) and $\text{C}(11)\text{--N}(2)$ (1.332(8) Å) distances are approximately equivalent and significantly shorter than the C–N single bond distances, indicating that the π -electrons of the C=N double

(20) (a) Giesbrecht, G. R.; Whitener, G. D.; Arnold, J. *J. Chem. Soc., Dalton Trans.* **1999**, 3601. (b) Chivers, T.; Parvez, M.; Schatte, G. *J. Organomet. Chem.* **1998**, 550, 213.

Table 4. Bond Lengths (Å) and Angles (deg) for **5**

Yb(1)–N(1)	2.244(5)	Yb(1)–C(10)	2.615(8)
Yb(1)–N(2)	2.284(5)	Yb(1)–C(7)	2.618(8)
Yb(1)–C(9)	2.589(8)	Yb(1)–C(6)	2.626(8)
Yb(1)–C(2)	2.589(8)	N(1)–C(11)	1.343(8)
Yb(1)–C(5)	2.593(8)	N(2)–C(11)	1.332(8)
Yb(1)–C(1)	2.597(8)	N(3)–C(18)	1.277(8)
Yb(1)–C(8)	2.602(8)	N(3)–C(11)	1.369(8)
Yb(1)–C(3)	2.604(8)	N(4)–C(18)	1.377(9)
Yb(1)–C(4)	2.607(8)	N(5)–C(18)	1.369(8)
N(1)–Yb(1)–N(2)	59.43(18)	N(2)–C(11)–Yb(1)	57.9(3)
C(11)–N(1)–Yb(1)	94.0(4)	N(1)–C(11)–Yb(1)	56.2(3)
C(11)–N(2)–Yb(1)	92.5(4)	N(3)–C(11)–Yb(1)	173.5(4)
C(18)–N(3)–C(11)	126.2(6)	N(3)–C(18)–N(5)	118.6(6)
N(2)–C(11)–N(1)	114.1(5)	N(3)–C(18)–N(4)	126.3(6)
N(2)–C(11)–N(3)	124.9(6)	N(5)–C(18)–N(4)	115.0(6)
N(1)–C(11)–N(3)	120.8(6)		

bond in the present structure are delocalized over the N–C–N unit.²¹ Consistent with this case, the Yb–N(1) and Yb–N(2) distances, 2.244(5) and 2.284(5) Å, are intermediate between the values observed for the Yb–N single bond distance and the Yb–N donor bond distances (2.19–2.69 Å),²² and are comparable to the corresponding values found in $(\text{C}_5\text{H}_5)_2\text{Yb}[(^i\text{PrNC}(\text{N}^i\text{Pr}_2)\text{N}^i\text{Pr}]]$ ($\text{Yb}_{\text{av}}\text{--N}$ 2.283(5) Å)^{10c} and $[(\text{CyN})_2\text{CN}(\text{SiMe}_3)_2]_2\text{YbN}(\text{SiMe}_3)_2$ ($\text{Yb}_{\text{av}}\text{--N}$ 2.317(13) Å).^{7b} In contrast with the observed delocalized C=N bond distance (N(2)–C(12) 1.305(6) Å) of the guanidine group $\text{N}=\text{C}(\text{NMe}_2)_2$ in **3**, the N(3)–C(18) bond distance (1.277(8) Å) in **5** is comparable to the value accepted for $\text{N}(\text{sp}^2)=\text{C}(\text{sp}^2)$ double bond (1.26 Å).¹⁵ The Yb–C(Cp) distances range from 2.585(8) to 2.619(7) Å, and are in the normal ranges observed for lanthanocene complexes. The average Yb–C(Cp) distance of 2.601(7) Å is similar to those found in other Cp_2Yb -containing compounds, such as $(\text{C}_5\text{H}_5)_2\text{Yb}(\text{PzMe}_2)$ – $(\text{HPzMe}_2)_2$, 2.62(1) Å;^{22a} $[(\text{C}_5\text{H}_5)_2\text{Yb}(\text{OCMe}=\text{C}=\text{CHMe})]_2$, 2.63(1) Å;^{22b} $(\text{C}_5\text{H}_5)_2\text{Yb}(\text{CH}_3)(\text{THF})$, 2.60(2) Å.^{22c}

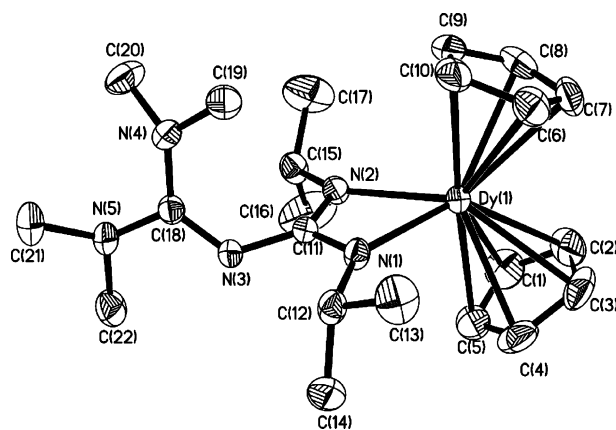


Figure 4. ORTEP diagram of **7** with the probability ellipsoids drawn at the 30% level. Hydrogen atoms omitted for clarity.

As shown in Figure 4, complexes **7** and **5** are isostructural. The structural parameters of **7** (Table 5) are very similar to

(21) Srinivas, B.; Chang, C.; Chen, C.; Chiang, M. Y.; Chen, I. T.; Wang, Y.; Lee, G. *J. Chem. Soc., Dalton Trans.* **1997**, 957.
 (22) (a) Zhou, X. G.; Huang, Z. E.; Cai, R. F.; Zhang, L. B.; Zhang, L. X. *Organometallics* **1999**, 18, 4128. (b) Zhou, X. G.; Wu, Z. Z.; Jin, Z. S. *J. Organomet. Chem.* **1992**, 431, 289. (c) Evans, W. J.; Dominguez, R.; Hanusa, T. B. *Organometallics* **1986**, 5, 263.

Table 5. Bond Lengths (Å) and Angles (deg) for **7**

Dy(1)–N(1)	2.291(3)	Dy(1)–C(3)	2.670(4)
Dy(1)–N(2)	2.331(3)	Dy(1)–C(7)	2.678(4)
Dy(1)–C(1)	2.648(4)	Dy(1)–C(6)	2.679(4)
Dy(1)–C(5)	2.651(5)	N(1)–C(11)	1.348(4)
Dy(1)–C(8)	2.654(4)	N(2)–C(11)	1.337(4)
Dy(1)–C(2)	2.654(4)	N(3)–C(18)	1.289(4)
Dy(1)–C(9)	2.659(4)	N(3)–C(11)	1.380(4)
Dy(1)–C(4)	2.659(4)	N(4)–C(18)	1.369(5)
Dy(1)–C(10)	2.669(4)	N(5)–C(18)	1.374(4)
N(1)–Dy(1)–N(2)	58.16(9)	N(2)–C(11)–Dy(1)	57.66(17)
C(11)–N(1)–Dy(1)	94.8(2)	N(1)–C(11)–Dy(1)	55.99(17)
C(11)–N(2)–Dy(1)	93.36(19)	N(3)–C(11)–Dy(1)	173.6(2)
C(18)–N(3)–C(11)	125.8(3)	N(3)–C(18)–N(4)	126.7(3)
N(2)–C(11)–N(1)	113.6(3)	N(3)–C(18)–N(5)	117.8(3)
N(2)–C(11)–N(3)	125.3(3)	N(4)–C(18)–N(5)	115.5(3)
N(1)–C(11)–N(3)	120.8(3)		

those found in complex **5**; the complex has no unusual distances or angles in the Cp₂Dy unit. The Dy–C(Cp) distances range from 2.648(4) to 2.679(4) Å. The average value of 2.660(4) Å is similar to those found in other Cp₂-Dy-containing compounds, such as [Cp₂Dy(OCMe=CHMe)]₂, 2.668(6) Å,^{23a} and [MeCpDy(η²-PzMe₂)(μ-O-SiMe₂PzMe₂)]₂, 2.684(16) Å.^{23b} The Dy–N distances of 2.291(3) and 2.331(3) Å are similar to the corresponding distances in complex **5**, when the difference in the metal ionic radii is considered.¹⁹

Conclusions

We synthesized the novel organolanthanide guanidinate complexes where the guanidinate ligands are coordinated in a μ-η¹:η²-fashion to rare earth metals. Further study on the

reactivities of these complexes to isocyanate and carbodiimide indicates that phenyl isocyanate readily monoinserts into the lanthanide–guanidinate ligand bonds of them under mild conditions; however, *N,N'*-diisopropylcarbodiimide cannot react with them under the same conditions. The results demonstrate that both the reaction activity of the insertion reagents and the bonding modes of the metal–ligand bonds strongly affect the insertion. Finally, we also first investigated the insertion of *N,N'*-diisopropylcarbodiimide into the lithium–nitrogen bond of LiN=C(NMe₂)₂, of which the insertion intermediate product can be used as a synthon to synthesize organolanthanide derivatives containing the guanidinoacetamidinate ligand.

Acknowledgment. We thank the National Natural Science Foundation of China and the Research Funds of Excellent Young Teacher, and the New Century Distinguished Scientist of National Education Ministry of China and the Research Funds of Excellent Doctor of Fudan University for financial support.

Supporting Information Available: Tables of atomic coordinates and thermal parameters, all bond distances and angles, and experimental data for all structurally characterized complexes. This material is available free of charge via the Internet at <http://pubs.acs.org>.

IC048683X

- (23) (a) Wu, Z. Z.; Xu, Z.; You, X. Z.; Zhou, X. G.; Huang, X. Y. *J. Organomet. Chem.* **1994**, 483, 107. (b) Zhou, X. G.; Ma, W. W.; Huang, Z. E.; Cai, R. F.; You, X. Z.; Huang, X. Y. *J. Organomet. Chem.* **1997**, 545–546, 309.